An undergraduate laboratory Mössbauer apparatus

A Sconza†, G Torzo†, G Calore†, A Loria‡, E Mazzega‡ and M Michelini‡

†Dipartimento di Fisica-Università di Padova, via Marzolo 8, 35131-Padova, Italy
‡Dipartimento di Fisica-Università di Modena via Campi 213, 41100-Modena, Italy

Abstract. A didactic apparatus is described that allows the measurement of Mossbauer absorption spectra using a home-made speed modulator, a commercial photodiode as gamma-detector, low cost home-made electronics and a low intensity radioactive source

Riassunto. Si descrive un apparato a carattere didattico misure di spettri di assorbimento Mossbauer basato su un modulatore di velocita autostruito, un fotodiodo commerciale come rivelatore dei raggi gamma, elettronica di basso costo in gran parte autocostruita ed una sorgente radioattiva di bassa intensita

1. Introduction

Performing a Mossbauer experiment can be very useful in teaching modern physics The student can be made familiar with such concepts as energy–momentum conservation laws, energy levels, linewidth, absorption and emission processes, the uncertainty principle and the Doppler effect

The experimental Mossbauer apparatus described here was designed for educational purposes and therefore its performance cannot be compared with that of much more expensive and complex commercial instruments, designed for research and industrial purposes However, it is not simply a demonstration apparatus it can be used for quantitative measurements of the Mossbauer effect A drawback is the rather long time required for data acquisition, owing to the manual operation This feature, on the other hand, may have a didactic value, bringing the student closer to the physics involved in the experiment than the commercial automatic systems Moreover, most of the devices employed in our apparatus may also be used for different experiments and some of them may even be assembled by the students themselves

2. The Mössbauer effect: a brief outline

Let us consider an excited free nucleus (i e not bound in a lattice) which is at rest with respect to the laboratory frame When it decays to the ground level by emitting a gamma ray, we know from the momentum and energy conservation laws that the photon cannot carry the whole available energy E_0, equal to the energy difference between the excited and the ground level A small fraction of this energy is taken by the nucleus which recoils with momentum $p_{nucleus} = p_r (= h\nu/c)$ The recoil energy is therefore $E_r = (p_r)^2/(2m) \simeq E_0^2/(2mc^2)$, and the photon energy is $E_r = E_0 - E_r$

Such a photon cannot be absorbed by a nucleus identical to the emitting one, because the required energy should be $E'_r = E_0 + E_r$, and the natural widths Γ of nuclear absorption and emission lines are very small for example with 14 4 keV gamma rays emitted by Fe^{57}, one has $\Gamma = 4.6 \times 10^{-9}$ eV ($\Gamma/E_r \simeq 3 \times 10^{-13}$), while the recoil energy $E_r \simeq 2 \times 10^{-3}$ eV is six orders of magnitude larger

Nuclear resonant fluorescence is therefore normally forbidden by the energy–momentum conservation laws†

Nuclear fluorescence, before the discovery of the Mossbauer effect, was made possible only by the artificial line broadening obtained by heating the source and/or the absorber (*Doppler thermal broadening*) (Metzger and Todd 1954), or by the line shifting obtained by moving the source and/or the absorber at very high speed (*Doppler shift*) (Moon and Storruste 1953)

A third possible way of obtaining nuclear gamma fluorescence was found by Rudolf Mossbauer (1958), who discovered the existence of atoms, embedded in suitable matrices, which have a finite probability of

---

† In contrast, atomic resonant fluorescence is easily observed because in this case $\Delta E \simeq 10^{-6}$ eV and $E_r \simeq 10^{-9}$ eV

almost perfectly recoil-free emission and absorption This may happen when the nuclei are strongly bound to the lattice both in the source and the absorber Using a classical physics picture one could say that in such cases everything happens as if the whole crystal mass replaces the mass of the recoiling nucleus in the expression of the recoil energy E_r A detailed treatment of the Mossbauer effect, however, requires an extensive discussion in the framework of the quantum mechanics that can be found in many classical textbooks (see, for instance, Frauenfelder 1962)

When identical nuclei of a particular kind that are bound to the same kind of lattice have zero relative velocity, resonant gamma absorption is observed The resonance will be destroyed by moving one nucleus with respect to the other with velocity v In fact the Doppler formula (neglecting small relativistic corrections), gives for the emitted gamma energy $E'_i = E_i(1 + v/c)$, where c is the speed of light and E_i is the photon energy when $v = 0$ It may be easily shown that a velocity v of a few millimeters per second is enough to shift a gamma line (e g 14 4 keV of Fe^{57}) by an amount equal to the full linewidth Γ $E'_i - E_i = E_i(v/c) \simeq 10^4(10^{-4}/10^8) \, eV = 10^{-8} \, eV \geqslant \Gamma$

A typical Mossbauer apparatus is sketched in figure 1 It consists of a source S, an absorber A, a speed modulator to produce the relative motion, a detector D and a counter C The gamma rays detected are those which have not undergone resonant absorption

The counting rate F, plotted versus the velocity v (transmission spectrum), in the present case of identical source and absorber, has a minimum at $v = 0$, and possibly other minima symmetric with respect to the central one, due to hyperfine splitting of the nuclear energy levels In the case of different emitter and absorber lattices, the shift from $v = 0$ of the central minimum measures the energy shift of the excited level in the nucleus of the target atom with respect to the same level of the nucleus in the source This is called isomeric shift and it depends on the physical-chemical nature of both the source and the absorber

The shift depends more generally on any interaction affecting the nuclei For example by using the

Mossbauer effect it has been possible to observe the gravitational red shift of the photon energy due to a height difference between source and absorber of a few tens of meters (Pound and Rebka 1960)

The existence of several minima is due to hyperfine interactions these produce a splitting of the excited level into symmetric sublevels It is, in fact, possible to observe the splitting due to the interaction of the nuclear quadrupole moment with the electric field gradient produced by the atomic electrons, and the splitting due to the interaction between the nuclear magnetic moment and a magnetic field (externally applied or produced by a ferromagnetic matrix)

3. Experimental apparatus

3.1. Speed modulator

In most commercially available Mossbauer spectroscopy apparatus a *constant acceleration* Doppler modulator is normally used In these devices the velocity grows linearly with time up to a maximum value v^+, and then it decreases linearly down to a negative maximum $v^- = -v^+$

Such a technique yields a full absorption spectrum for each cycle, provided that the number of detected gamma quanta is high enough It requires, however, a complex and expensive apparatus consisting of a constant acceleration driver (Seberini 1988) plus multichannel analyser, that may not be immediately understood by the student

We preferred the simpler solution of a *constant velocity* drive here the spectrum is built up, point by point, by measuring the γ counts accumulated during the motion at a given velocity, and by changing the velocity after each counting period This method drastically reduces both the cost and the complexity of the data acquisition system One needs only a discriminator that selects the pulses of amplitude corresponding to the gamma quanta of interest, a timer that measures the acquisition time and a counter which records the pulses

In our apparatus the source is at rest and the absorber is attached to the moving frame The constant speed motion is obtained using a trolley driven by a worm-gear (see figure 2) The screw is 30 cm long with 2 5 mm pitch The absorber holder is mounted on low noise cylindrical ball bearings sliding on two steel rods The constant angular velocity of the worm-gear is provided by a feedback control in the circuit which drives the DC motor (0–12 V with a maximum current of 2 A) The feedback is produced by a second (coaxial) small motor which acts as a tachimetric dynamo The speed can be continuously adjusted by means of a potentiometer which sets a reference voltage for the driving motor the signal generated by the dynamo is used as a 'correction' to the reference voltage so that, after a short transient the speed is stabilized by the closed loop A *soft* mech-

Figure 1 A sketch of the Mossbauer experiment S is the gamma source, A the absorber, D the detector and C the counter The Mossbauer absorption spectrum is obtained by plotting the counting rate F of the detected gamma versus the velocity v of the absorber
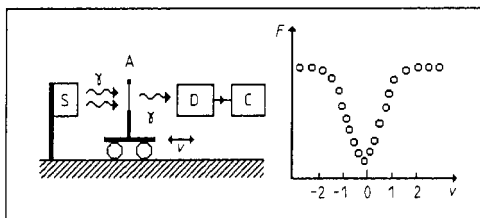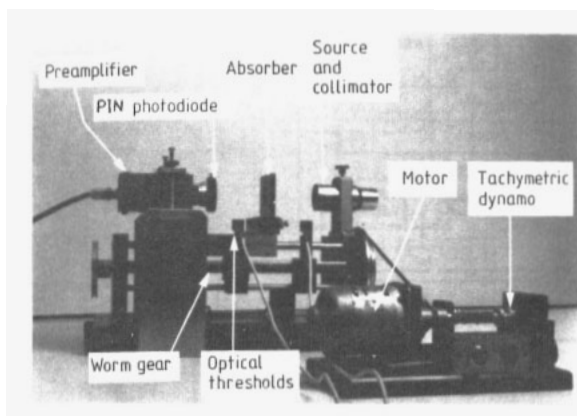
Figure 2. The mechanics of the speed modulator. The cobalt source is placed in a cylindrical lead–aluminium collimator. The PIN photodiode is protected from the ambient light by means of a thin aluminium foil and it is directly attached to the preamplifier. The moving absorber-holder has a shutter that intercepts the light beam at the optical thresholds.

anical coupling between the motor and the worm-gear, as well as a suitable speed reduction, is provided by rubber bands on pulleys. Some care must be paid to shield the trolley from the vibration produced by the motor: a good choice is to place the motor on a separate table.

The trolley drifts along a track where two optical detectors are placed to give the START and STOP signals to the electronic clock and to the pulse counter. To avoid the transient, a proper delay is provided to the START signal after the forward motion has started. The clock and the counter are disabled just before inverting the motion direction, and the backward speed is reset to a maximum value ($\simeq 1\,\mathrm{cm\,s^{-1}}$) to reduce the total acquisition time. These features facilitate performing repeated sweeps at the same speed, in order to increase the statistics of the count rate.

The trolley speed $v = d/t$ is obtained for a fixed distance d between the two optical thresholds by measuring the drift time t. The detailed circuitry is shown in figure 3. The material required for building the mechanical part of the constant-velocity drive has a value of a few hundred dollars (precise worm-gear, bearings, motor...), but the device should be made by expert technicians in a well equipped mechanical shop. An alternative solution is a commercial trolley whose price is of the order of $1 500.†

The accuracy of our device was tested using a digitizer with a resolution of 10^3 steps/turn to measure the stability of the worm-gear angular velocity during the whole sweep: in figure 4 we show, as a function of the trolley speed, the relative standard deviation of

† For example: Linear Positioner, produced by Physik Instrumente Gmbh, Siemensstrasse D-7517 Waldbronn, Germany.

the distribution of the time intervals between successive steps of the digitizer. With a pulley-radius ratio (speed reduction) of 1/10, the velocity fluctuations are smaller than 0.2%, except for the smallest velocities. In this case it is worth increasing the speed reduction (e.g. radius ratio 1/40).

3.2. Source and absorber

The most common Mössbauer sources commercially available are $_{27}\mathrm{Co}^{57}(\rightarrow\,_{26}\mathrm{Fe}^{57})$, $_{62}\mathrm{Sm}^{151}(\rightarrow\,_{61}\mathrm{Eu}^{151})$, $_{50}\mathrm{Sn}^{119}$, $_{74}\mathrm{W}^{182}(\rightarrow\,_{73}\mathrm{Ta}^{182})$ and $_{53}\mathrm{I}^{127}(\rightarrow\,_{52}\mathrm{Te}^{127})$. Among these, at room temperature, Co^{57} is usually preferred because it offers high fraction of recoilless emission (70%). The radioactive element may be embedded into a Cr, Cu, Pd, Pt, Fe or Rh matrix.

We used a nearly exhausted source of cobalt-rhodium donated by a Mössbauer spectroscopy laboratory because it had reached the end of its useful life. The original intensity was 100 mCi and, with a half-life of 271 days, after a few years use, the actual intensity could be evaluated to be approximately 1 mCi. The ability to use a very weak source in a tutorial Mössbauer experiment is a very important feature, not only for economical reasons (a standard source costs more than $1000), but also for safety reasons, as it reduces the possible damage due to an accidental exposure.

The main emission lines of this source are 14.4 keV (9%), 122 keV (86%), 136.3 keV (11%)‡, plus 6.4 keV x-rays (K_α line from $_{26}\mathrm{Fe}^{57}$). The Mössbauer line is at 14.4 keV, with a natural width $\Gamma \simeq 5 \times 10^{-9}\,\mathrm{eV}$, or in terms of Doppler shift $\Delta v \simeq 0.1\,\mathrm{mm\,s^{-1}}$. The effective width depends on various features such as matrix type, intensity, age etc.

We used as an absorber a stainless steel foil (25 μm thick). Stainless steel associated to the Co-Rh source offers the great simplification of a Mössbauer spectrum without line splitting. Alternative absorbers of didactic interest are natural iron which shows six absorption lines due to magnetic splitting, and $\mathrm{Na_2Fe(CN)_5NO.2H_2O}$ which shows the quadrupole splitting. The time needed to obtain such spectra with sufficient resolution is, however, extremely long using our low-intensity Co source.

3.3. Detector and amplification chain

The gamma detectors most widely used in Mössbauer spectroscopy are the proportional counters, usually filled with argon or xenon (97%) and CO_2 or CH_4 (3%) and biased at nearly 2 kV. These detectors cost

‡ The $_{27}\mathrm{Co}^{57}$ nucleus decays to $_{26}\mathrm{Fe}^{57}$ by electron capture (inverse beta decay). The excited Fe nucleus decays to the ground level by emitting a 136.3 keV gamma ray (11% of the cases) or it decays to an excited level at 14.4 keV by emitting a 122 keV gamma ray. The latter de-excites principally by transferring its energy to the atomic electrons (electron conversion) or (only in 9.5% of the cases) by gamma ray emission.
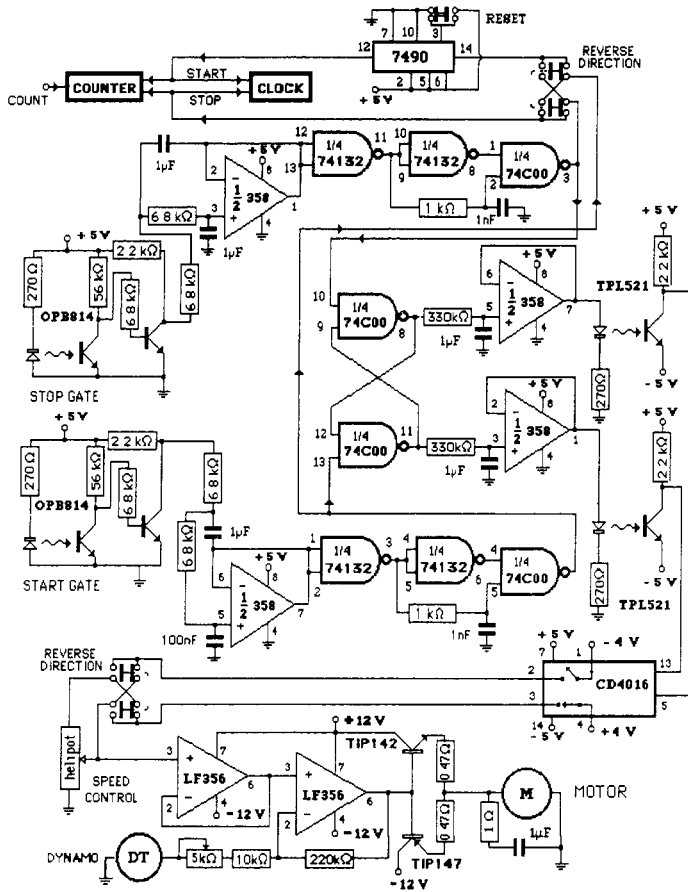
Figure 3. The complete circuitry for the speed modulator. The start and stop signals produced by the optocouplers OPB814 trigger the counter and clock as well as the switching between forward and backward motion. Repeated measurements at a fixed speed can be performed automatically. The speed value is adjusted through a potentiometer, while its sign (positive for source approaching the absorber) is controlled by a twin (two-way four-pole) switch.

Figure 4. A measurement of the stability of the worm-gear angular velocity. The trolley is driven by our feedback-controlled motor and a digitizer is attached to the worm gear. Full circles: speed reduction = 1/10. Open circles: speed reduction = 1/40.
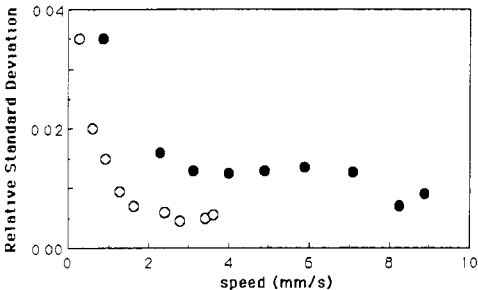
about $2000, excluding the high-voltage power supply. Also frequently used are semiconductor detectors (Ge or Si) which offer very high resolution if they are kept at liquid nitrogen temperature (Wertheim 1967); these are very expensive too.

We adopted a much simpler and cheaper solution: a silicon PIN photodiode[†] which works at low bias voltage (10–30 V) and at room temperature. It is a recently developed device that has not yet been extensively used in nuclear physics experiments. Its main features are: fast response, good efficiency for low energy gamma rays, sufficient detecting area (1 cm²).

The photodiode has the structure shown in figure

[†] Hamamatsu, model S-1723 06 ($\approx$ $100). For a detailed description of this photodiode see Yamamoto *et al* (1987). See also Bilton (1988).

$$di_1^2 = \frac{2kT}{\pi R_t}\,d\omega \qquad di_2^2 = \frac{eI_d}{\pi}\,d\omega \qquad dv^2 = \frac{2kT}{\pi}\left[\frac{2}{3g_m}+R_d\right]d\omega$$

$$R_t = R\,\text{bias} \,\|\, R_f \qquad C_t \approx C_{diode} + C_{FET} + C_{parasitic}$$
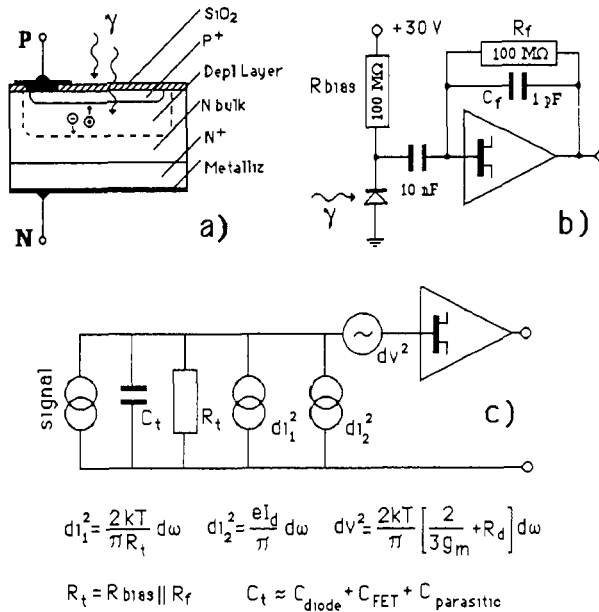
Figure 5. (a) The PIN photodiode structure ○ (b) Schematic of the detector circuitry photodiode and charge-preamplifier (c) Equivalent noise circuit as seen at the preamplifier FET input

5(a) It is obtained from high-resistivity ultrapure n-doped silicon wafers (200 μm thick) using the planar process technique described for instance by Kemmer (1982, 1984)

When it is reverse-biased by a voltage, U, the depletion layer thickness d is given, in μm, by the relation $d = 0.5\sqrt{\rho U}$, where ρ is in ohm cm, and U in volts The bias voltage cannot exceed 30 V, and the resistivity is $\rho \simeq 3\,500$ ohm cm The maximum thickness of the depletion layer is therefore $d \simeq 150\,\mu$m

Each photon absorbed within the depletion layer transfers its energy to a single electron[†] which generates a number of electron–hole pairs proportional to the photon energy (on average the energy loss is 3.6 eV/pair in silicon) These electron–hole pairs are quickly swept to the collecting electrodes by the junction–barrier electric field The typical pulse rise time is about 15 ns

The thicker the depletion layer the greater is the photodiode efficiency The mass absorption coefficient for gamma rays of 14.4 keV is $\simeq 2.8 \times 10^{-3}\,\mu m^{-1}$, and therefore with a depletion layer thickness of 150 μm, the efficiency is expected to be $\simeq 35\%$ at 14.4 keV (to be compared with $\simeq 86\%$ for a Xenon proportional counter for gamma rays of the same energy) It drops to less than 1% at 122 keV

[†] Mainly by photoelectric effect at low energy, or by Compton effect or direct pair production at higher energy All these electrons lose their kinetic energy E_k within the depletion layer for $E_k \leqslant 50$ keV their range in silicon is less than 10 μm

The energy resolution of the detector depends essentially on the electronic noise of the amplifier chain This is made of a FET input charge-preamplifier (figure 5(b)) which converts the collected charge into a voltage pulse (typical rise time of 15 ns and decay time of 10–100 μs), followed by a pulse shaping amplifier

The noise depends principally (see appendix) on the total input capacity (mostly due to the photodiode capacity), on the equivalent input resistance (i e the parallel of the diode bias resistance and of the charge-amplifier feedback resistance), and on the FET transconductance It also depends on the kind of shaping performed by the amplifier and on its shaping time

In our set-up we can predict a minimum equivalent noise charge $\text{ENC} \simeq 400$ electrons, corresponding to an energy resolution $\text{FWHM} \simeq 3.4$ keV

We used both commercial pulse-shaping circuitry[‡], and much cheaper circuitry consisting of a hybrid circuit preamplifier[§] plus a home-made Gaussian shaper, whose details are given in the appendix

The measured resolution of our detector is about

[‡] Made of Silena preamplifier, model CSTA1 plus Ortec shaper, model 572 (Gain = 1500, shaping time = 2μs) total cost $\approx$ \$2000
[§] Laben, model 5254 ($\approx$ \$20) It has been developed for the DELPHI experiment at the LEP accelerator at CERN (see Barichello *et al* 1987)
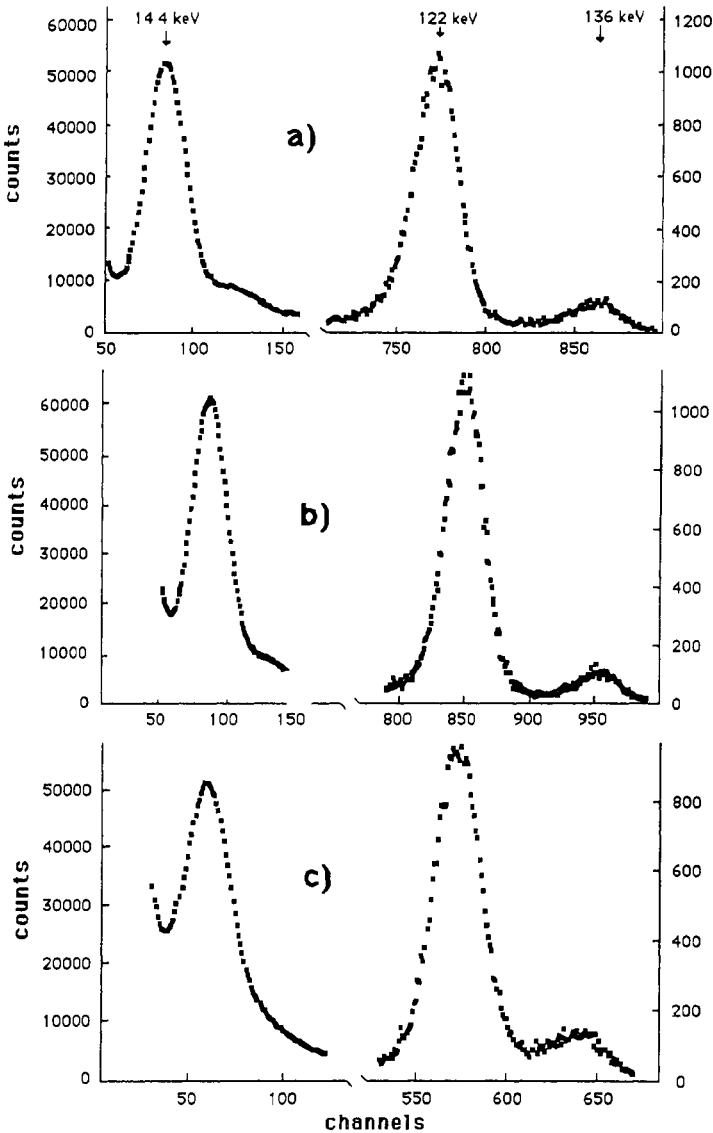
Figure 6 The source emission spectrum obtained with (a) preamplifier Silena CSTA1 plus shaper Ortec 572 (shaping time = $2\,\mu$s), (b) preamplifier CSTA1 plus our shaper, (c) hybrid circuit Laben 5254 preamplifier plus our shaper

4 keV FWHM both at 14 4 keV and 122 keV, as shown in figure 6, where a Co^{57} spectrum obtained with a multichannel analyser Silena 7922 is reported In figure 6(a) the data were taken using the commercial amplifier chain (Silena CSTA1 preamplifier and Ortec 572 shaper) The data shown in figure 6(b) were taken replacing the Ortec amplifier with our home-made

five-pole shaper, obtaining practically the same resolution

The cheapest version is offered by the hybrid circuit Laben preamplifier followed by our five-pole shaper The performance of this set-up is about 25% worse (figure 6(c)) than the previous ones, but it is still sufficient for our purposes
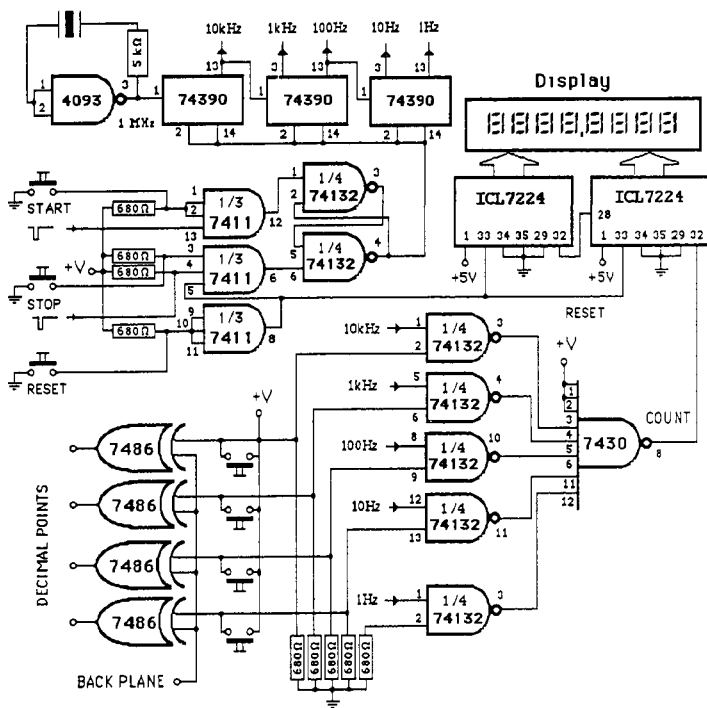
Figure 7 The clock circuitry

3.4. Discriminator, clock and counter (single channel analyser)

The pulses generated by the detector must be filtered by a pulse-height discriminator which feeds to the counter only the signals whose amplitude V_x satisfies the relation $V - \frac{1}{2}\Delta V < V_x < V + \frac{1}{2}\Delta V$, where V is the amplitude corresponding to the 14 4 keV photon peak maximum We built a pulse-height discriminator circuit (Parker and French 1985) that is both cheap and simple It allows independent adjustments of the window width ΔV and of the window height V, thus making the calibration procedure easier

The calibration is essentially a measurement of the source emission spectrum This is accomplished by recording the counting rate as a function of the window height

The acquisition time is measured by a simple home-made electronic clock This is made from two ICL7224 counters, driven by a 1 MHz quartz oscillator through a chain of 'divide by ten' circuits, as shown in figure 7

The counter is also made from a single integrated circuit ICL7224, which drives a $4\frac{1}{2}$ digit liquid crystal display

The Co^{57} spectrum shown in figure 8 was taken using the pulse-height discriminator, the hybrid circuit preamplifier and the home-made counter and clock

4. Experimental procedure and results

The experiment consists of two parts (i) the detector calibration, (ii) the Mossbauer absorption spectrum measurement

The calibration is performed, without absorber, by detecting the 122 keV and 14 4 keV peaks of the cobalt source This requires nearly half an hour of acquisition (e g thirty values for the discriminator voltage threshold V, one minute of acquisition each,

Figure 8 The source emission spectrum, measured using the single-channel discriminator, the hybrid-circuit preamplifier and the home-made counter and clock The acquisition time for each voltage setting was 1 min in the low-energy region and 5 min in the high-energy region
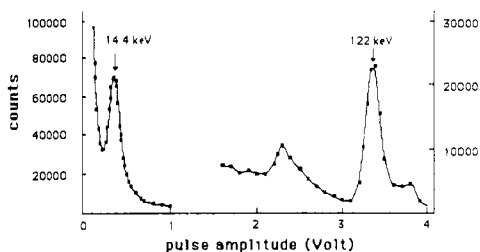
with a rather narrow window width ΔV) Once the 14 4 keV peak is identified, V is set to the value corresponding to the peak maximum, and ΔV is adjusted to select the 14 4 keV line

The acquisition of the Mossbauer spectrum is then carried out with the absorber placed on the trolley The speed for each sweep is selected using the helipot shown in figure 3 A single sweep gives sufficient statistics at low speed, while multiple sweeps must be performed at the higher speed values Once the acquisitions for $v < 0$ (i e with the absorber approaching the source) are finished the direction of motion is reversed This function is performed using the two reversing switches (reverse direction in figure 3) that control the START and STOP signals and the speed-control voltage signals At this point new values are selected for the speed and the acquisitions for $v > 0$ are completed

The Mossbauer absorption spectrum shown in figure 9 was obtained with a 25 μm thick stainless steel absorber using the hybrid-circuit preamplifier, our five-pole shaper, and the pulse-height discriminator The distance between the start and stop thresholds was 25 mm, with a source-to-detector distance of 200 mm, thus making the errors due to the finite solid angle seen by the detector negligible The experimental data are well fitted by a Lorentzian curve centred at $v = -0\,209 \pm 0\,005$ mm s^{-1}, with half-width $\Gamma \simeq 0\,453 \pm 0\,015$ mm s^{-1} These are the values usually obtained for a cobalt in rhodium matrix with stainless steel absorber (the Mossbauer linewidth is the sum of the emission and absorption linewidths, plus the line broadening due to the source ageing)

All the features of the apparatus here described are aimed at maximizing the learning opportunities and minimizing the overall costs Its modular design should help the understanding of the single parts,

Figure 9 The Mossbauer transmission spectrum of a 25 μm thick stainless steel absorber obtained with the hybrid-circuit preamplifier, our five-pole shaper, and the pulse-height discriminator
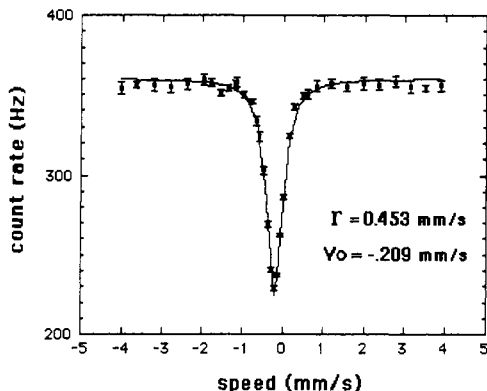
while offering the possibility of using the single blocks in complementary activities (e g source spectra measurements, analysis of solid state detector characteristics etc) A special effort has been made to give to the students the opportunity of building up most of the electronics by themselves, not as 'black-box' assembling, but with the aim of understanding the function and performance of each device

Appendix. Noise evaluation and Gaussian shaper design

The principle noise sources in the detector–preamplifier circuitry shown in figure 5 are (Nicholson 1974) the *shot noise* of the diode reverse bias current ($I_d \simeq 1\,5$ nA), and the *Johnson noise* of the diode series resistance ($R_d \simeq 7\,\Omega$), of the equivalent resistance of the FET channel ($R_{eq} = 2/3 g_m$, where g_m is the FET transconductance), and of the feedback resistance ($R_t = 100$ MΩ) in parallel with the bias resistance ($R_{bias} = 100$ MΩ)

From the equivalent circuit of figure 5(c), assuming $1/\omega C_t \ll R_t$, the total voltage noise at the preamplifier input may be shown to have the form

$$(dV_{ni})^2 = [a^2 + (b/\omega)^2]d\omega$$

where

$$a^2 = \frac{4kT}{2\pi}\left[\frac{2}{3g_m} + R_d\right] = \frac{4kT}{2\pi}R_s \qquad (\text{'series noise'})$$

and

$$b^2 = \frac{4kT}{2\pi C_t^2}\left[\frac{1}{R_t} + \frac{eI_d}{2kT}\right] = \frac{4kT}{2\pi}\frac{1}{C_t^2 R_p}$$

(‘parallel noise’)

with k = Boltzmann constant, T = absolute temperature and e = electronic charge

The total input capacity is $C_t = C_{FET} + C_{parasitic}$, where C_{FET} is the FET gate capacity (typically 10 pF), and the diode junction capacity may be evaluated as $C_d = \varepsilon_0\varepsilon_r A/d$, where $A \simeq 1$ cm^2 is the junction area, and $\varepsilon_r = 12$ is the relative dielectric constant of Si) With a depletion layer thickness $d \simeq 150$ μm the diode contribution results to be predominant ($C_d \simeq 70$ pF) giving a total capacity $C_t \simeq 100$ pF
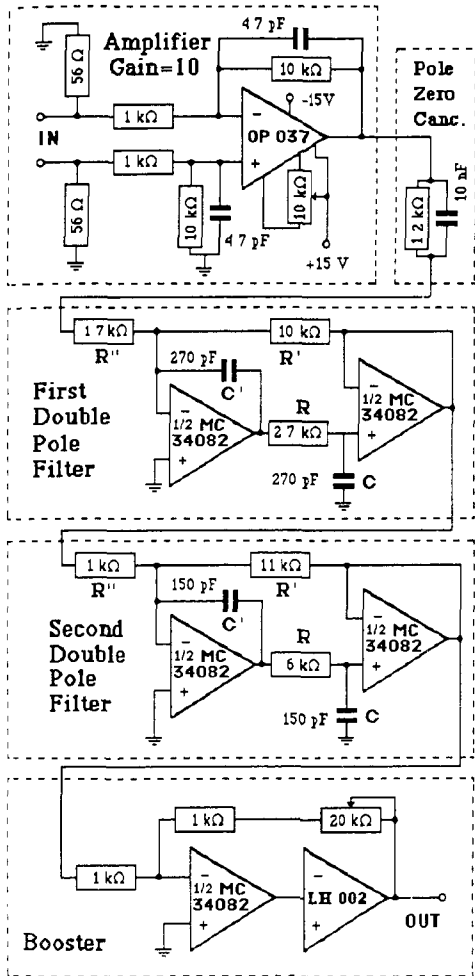
Figure 10 Complete circuitry of the five-pole Gaussian shaper technical details are explained in the text

The equivalent input resistance is $R_i = R_{bias} \| R_f = 50\,M\Omega$, and assuming the typical value $10^{-2}\,\Omega^{-1}$ for g_m we obtain $R_s \simeq 75\Omega$, $R_p \simeq 20\,M\Omega$

The voltage noise at the output of the shaper amplifier $(V_{no})^2$ is a function of the shaping time τ with a minimum for $\tau \simeq \tau_c = a/b$, for most of the usual shaping forms In our case $\tau_c = C_i\sqrt{R_s R_p} \simeq 3\,9\,\mu s$

The minimum equivalent noise charge (ENC_{min}) may be computed from the relation $(ENC_{min})^2 \simeq F^2 C_i^2 2\pi ab = 4kTF^2 C_i \sqrt{R_s/R_p}$, where F is a 'demerit' factor whose value is 1 in the ideal case of cuspid-like shaping

We used a Gaussian shaping which gives an F value only 12% larger than unity, and therefore an

$ENC_{min} \simeq 400$ (electrons) corresponding to a predicted energy resolution (expressed as 'full width at half maximum') $FWHM = 2\sqrt{2\ln 2} \times 0\,36 \times ENC \simeq 3\,4\,keV$
As shown by Ohkawa et al (1976), an approximately Gaussian shaping is obtained when the amplifier transfer function has the form $H(s) = H_0/Q^{(n)}(s)$, where $Q^{(n)}(s)$ is a n-order Hurwitz polynomial with an appropriate series of complex conjugate poles $A_i \pm jW_i$ (plus a real pole A_0 if n is odd) The Gaussian approximation improves with the order of the polynomial $Q^{(n)}(s)$, and it is good enough for $n = 5$

Our shaper is shown in figure 10 It has an input amplifier stage (gain = 10, no shaping) followed by a pole-zero cancellation circuit that transforms the real pole of the preamplifier into the Ohkawa A_0 pole This circuit is followed by two active filters each providing a complex conjugate pole pair, plus an output booster stage

The time constants RC and $R'C'$ are determined by the Ohkawa conditions on the poles

$$A_i = \frac{\sigma}{2RC} \qquad \text{and} \qquad W_i = \frac{\sigma}{2RC}\left(\frac{4RC}{R'C'} - 1\right)^{1/2}$$

where σ is the width of the Gaussian output signal $V = V_0 \exp(-t^2/2\sigma^2)$ The A_i, W_i for $n = 5$, and the σ optimum value have been calculated to be $A_0 = 1\,476$, $A_1 = 1\,417$, $W_1 = 0\,598$, $A_2 = 1\,204$, $W_2 = 1\,299$ and $\sigma = 0\,73\,\tau_c$ respectively

Each active filter gain may be adjusted by changing the resistance R'', without affecting the poles position The shaper overall gain $(\simeq 10^3)$ may be further regulated by trimming the feedback resistance in the booster stage

References

Barichello G et al 1987 Nucl Instrum Methods A **254** 111
Bilton C, Hedges S, Holson P R and Imrie D C 1988 J Phys E Sci Instrum **21** 809
Frauenfelder H 1962 The Mossbauer Effect (New York Benjamin Inc)
Kemmer J 1982 IEEE Trans Nucl Sci **NS29** 733
——1984 Nucl Instrum Methods **226** 89
Metzger F R and Todd W B 1959 Phys Rev **95** 853
Moon P B and Storruste A 1953 Proc Phys Soc A **66** 585
Mossbauer R 1958 Z Phys **151** 124
Nicholson P W 1974 Nuclear Electronics (New York John Wiley)
Ohkawa S, Yoshizawa M and Husimi K 1976 Nucl Instrum Methods **138** 85
Parker R H and French J D 1985 Am J Phys **53** 793
Pound R V and Rebka G A 1960 Phys Rev Lett **4** 337
Seberini M 1988 J Phys E Sci Instrum **21** 641 and references therein
Wertheim G K 1967 Phys Today **31** See for example the GLP and SLP detectors produced by EG & G-Ortec
Yamamoto K et al 1987 Nucl Instrum Methods A **253** 542